

Structural Gender Dimorphism and the Biomechanics of the Gluteal Subcutaneous Tissue: Implications for the Pathophysiology of Cellulite

Christina Rudolph, B.A.
Casey Hladik, B.A.
Hassan Hamade
Konstantin Frank, M.D.
Michael S. Kaminer, M.D.
Doris Hexsel, M.D.
Robert H. Gotkin, M.D.
Neil S. Sadick, M.D.
Jeremy B. Green, M.D.
Sebastian Cotofana, M.D.,
Ph.D.

Albany and New York, N.Y.; Munich, Germany; Chestnut Hill, Mass.; Porto Alegre, Brazil; and Coral Gables, Fla.

Background: This study was performed to investigate gender differences in gluteal subcutaneous architecture and biomechanics to better understand the pathophysiology underlying the mattress-like appearance of cellulite.

Methods: Ten male and 10 female body donors [mean age, 76 ± 16.47 years (range, 36 to 92 years); mean body mass index, 25.27 ± 6.24 kg/m² (range, 16.69 to 40.76 kg/m²)] were used to generate full-thickness longitudinal and transverse gluteal slices. In the superficial and deep fatty layers, fat lobule number, height, and width were investigated. The force needed to cause septal breakage between the dermis and superficial fascia was measured using biomechanical testing.

Results: Increased age was significantly related to decreased dermal thickness, independent of sex (OR, 0.997, 95 percent CI, 0.996 to 0.998; $p < 0.0001$). The mean number of subdermal fat lobules was significantly higher in male body donors (10.05 ± 2.3) than in female body donors (7.51 ± 2.7 ; $p = 0.003$), indicating more septal connections between the superficial fascia and dermis in men. Female sex and increased body mass index were associated with increased height of superficial fat lobules. The force needed to cause septal breakage in male body donors (38.46 ± 26.3 N) was significantly greater than in female body donors (23.26 ± 10.2 N; $p = 0.021$).

Conclusions: The interplay of dermal support, septal morphology, and underlying fat architecture contributes to the biomechanical properties of the subdermal junction. This is influenced by sex, age, and body mass index. Cellulite can be understood as an imbalance between containment and extrusion forces at the subdermal junction; aged women with high body mass index have the greatest risk of developing (or worsening of) cellulite. (*Plast. Reconstr. Surg.* 143: 1077, 2019.)

Cellulite is considered an aesthetic condition associated with profound feelings of body dissatisfaction, psychosocial stress, and decreased quality of life¹⁻³ that affects post-pubertal female subjects (80 to 98 percent) of

all ages and ethnicities.⁴⁻¹² It is characterized by a mattress-like skin appearance, most commonly affecting the buttocks and posterior thigh.^{9,12-15} Although different pathophysiologic models have been proposed, including vascular/inflammatory,^{4,12,16-19} hormonal,^{10,20,21} and structural^{5,22-26} causes, the complete understanding of cellulite remains elusive.

From the Department of Medical Education, Albany Medical College; the Department for Hand, Plastic and Aesthetic Surgery, Ludwig Maximilians University; Skincare Physicians; the Brazilian Center for Studies in Dermatology; Private practice; the Department of Dermatology, Weill Medical College of Cornell University; and Skin Associates of South Florida.

Received for publication June 7, 2018; accepted September 12, 2018.

Copyright © 2019 by the American Society of Plastic Surgeons

DOI: 10.1097/PRS.0000000000005407

Disclosure: The authors have no commercial associations or financial disclosures that might pose or create a conflict of interest with the methods applied or the results presented in this article. This study received funding from Merz North America, Inc., Raleigh, N.C. (grant no. 02092018).

Previous studies investigating cellulite using anatomical dissections^{5,22,25} and high-resolution magnetic resonance imaging^{23,27} have reported on gender differences in the subcutaneous architecture, with male subjects having obliquely oriented, highly interconnected subdermal connective fibers and female subjects having less densely arranged, perpendicularly arranged fibers. It has been proposed that these structural differences seen in female subjects provide less stability to the overlying skin, thereby making female subjects more prone to skin retraction at septal-dermal attachment points.^{5,22–25,27,28} This may be further exacerbated by septal fibrosis secondary to various hormonal and inflammatory factors^{6,17,26,29} and has been postulated to cause the dimpled skin appearance in cellulite.^{25,28,30}

Although several studies have sought to provide conclusive evidence on gender differences in the anatomical structural arrangement, these investigations should be interpreted with caution. These studies were limited because of small sample size,^{22,27,28} including female subjects without having a representative comparison group,^{5,22,23,25,28} or failure to correlate anatomical subcutaneous architecture to its underlying biomechanical properties.^{5,22–25,27,28} Thus, the connection between structure and function underlying cellulite pathophysiology has not been fully elucidated.

The objectives of this study were to (1) report on gender differences in the architectural arrangement of the gluteal subcutaneous tissue

(i.e., the number, height, and width of the fat lobules, and the number of septal connections), (2) measure the thickness of the dermis and the superficial and deep fatty layers, (3) measure the force required to cause septal breakage in the superficial fatty layer, and (4) correlate the above parameters to age and body mass index in 10 male and 10 female body donors.

MATERIALS AND METHODS

Study Sample

We investigated a representative sample of 20 fresh cadavers from 10 male and 10 female Caucasian body donors with a mean age of 76 ± 16.47 years (range, 36 to 92 years) and a mean body mass index of 25.27 ± 6.24 kg/m² (range, 16.69 to 40.76 kg/m²) (Table 1). The cadavers were not clinically assessed for cellulite before death. While alive, all body donors gave their informed consent for their bodies to be used after death in medical education and research. No donors had previous surgical interventions or diseases affecting the physical or mechanical integrity of the gluteal structures.

Anatomical Dissections

Full-thickness incisions of each gluteal region ($n = 40$) were executed, including the following layers: dermis, superficial fat (fatty layer between dermis and superficial fascia), superficial fascia, deep fat (fatty layer between superficial fascia

Table 1. Gender Differences of the Measured Parameters of the Honeycomb-Like Arranged Lobules in a Single Row Located in the Most Superficial Layer of the Superficial Fat and in a Single Row Located in the Most Superficial Layer of Deep Fat*

	Male	Female	<i>p</i>
No. of specimens	20	20	—
Age, yr	76.6	75.4	0.823
BMI, kg/m ²	22.24	28.29	0.002†
Mean dermis thickness ± SD, cm	0.17 ± 0.07	0.17 ± 0.08	0.903
Between the dermis and the superficial fascia			
Mean distance from the dermis to the superficial fascia ± SD, cm	0.58 ± 0.23	0.88 ± 0.44	0.011†
Mean no. of honeycombs per area in the superficial layer ± SD	10.1 ± 2.28	7.50 ± 2.69	0.003†
Mean height of honeycombs in the superficial layer ± SD, cm	0.23 ± 0.09	0.36 ± 0.13	0.001†
Mean width of honeycombs in the superficial layer ± SD, cm	0.32 ± 0.09	0.44 ± 0.13	0.001†
Mean ratio of width to height of honeycombs in the superficial layer ± SD	1.48 ± 0.53	1.32 ± 0.47	0.294
Between the superficial fascia and the deep fascia			
Mean distance from the superficial fascia to the deep fascia ± SD, cm	1.00 ± 0.45	1.49 ± 0.58	0.005†
Mean no. of honeycombs in the deep layer ± SD	5.06 ± 1.38	4.42 ± 1.44	0.158
Mean height of honeycombs in the deep layer ± SD, cm	0.39 ± 0.19	0.58 ± 0.30	0.022†
Mean width of honeycombs in the deep layer ± SD, cm	0.65 ± 0.25	0.76 ± 0.28	0.207
Mean ratio of width to height of honeycombs in the deep layer ± SD	1.84 ± 0.59	1.75 ± 1.52	0.814
Mean force to cause septal breakage ± SD, N	38.46 ± 26.3	23.26 ± 10.20	0.021†

BMI, body mass index.

*Two specimens (longitudinal and transverse gluteal slices) were obtained from each body donor. Values are given as mean ± SD. Independent *t* tests were computed to investigate difference between male and female measurements.

†Statistically significant.

and deep fascia), deep fascia (the investing fascia of the gluteus maximus muscles), and gluteus maximus muscle. In all cadavers, the superficial fascia was a substantial layer of dense fibrous connective tissue that separated the superficial fat from the deep fat (Fig. 1). The fat was arranged in lobules of different sizes, thereby resembling a honeycomb.

To study the fat lobule architecture, two 5-cm-long, full-thickness incisions of the prone-positioned body donors were made in a longitudinal (9 cm lateral from midline) and a transverse (5 cm from midline) orientation at the coccygeal-sacral fusion level (Fig. 2). All body donors were objectively dissected according to scientific research ethics at the Department of Medical Education, Albany Medical College, Albany, New York.

Gluteal Slice Image Analysis

To investigate the fat lobule and connective tissue architecture, photographs were immediately taken after making both full-thickness incisions without disturbing the *in vivo* structure. Photographs were transferred to a workstation and analyzed digitally using ImageJ software (National Institutes of Health, Bethesda, Md.). The following structural parameters were analyzed:

1. Dermal thickness (in millimeters): the distance from the undersurface of the epidermis to the margin of the hypodermis and superficial fatty layer.
2. Number (count), height, and width of fat lobules (in millimeters): the number, height, and width of fat lobules in a single

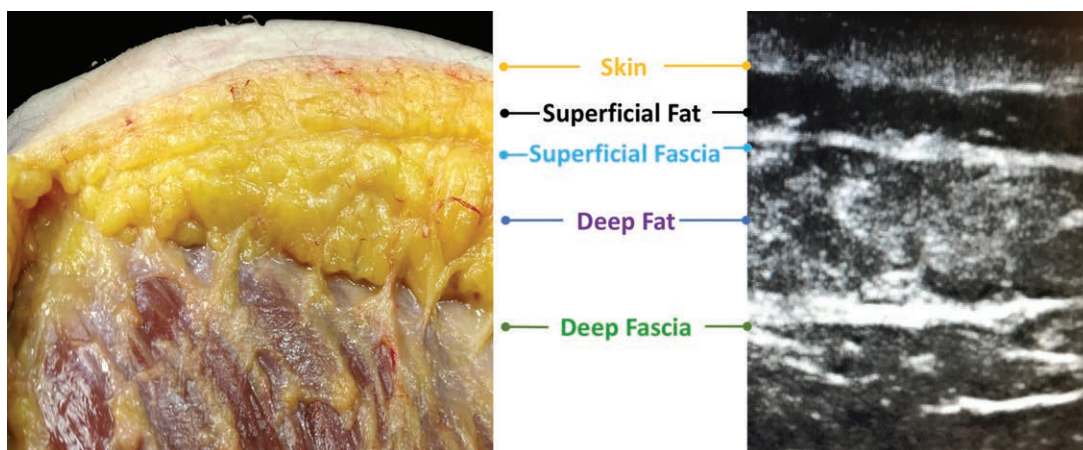


Fig. 1. Layered arrangement of the subdermal gluteal region of a female body donor in a photograph of a longitudinal slice (*left*) and an ultrasound image (*right*). From superficial to deep, the layered arrangement consists of the skin, superficial fat, superficial fascia, deep fat, and deep fascia.

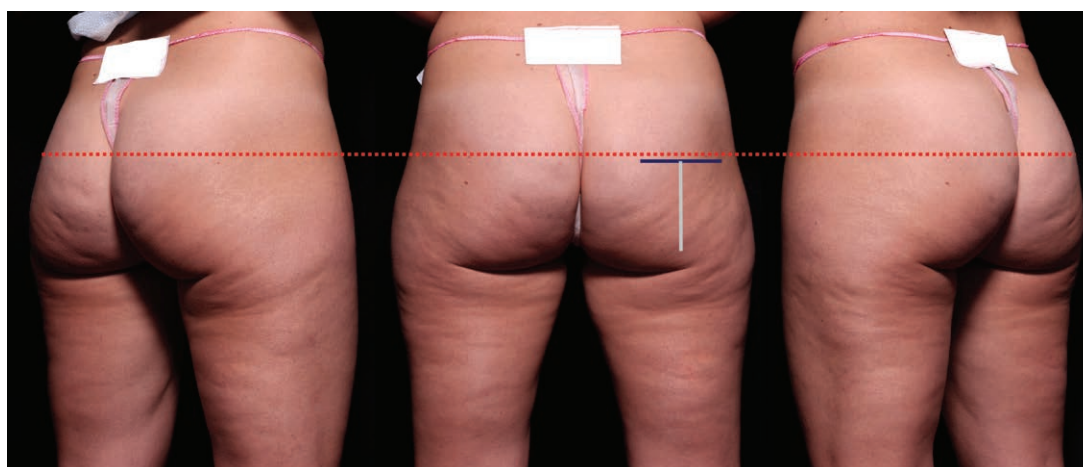


Fig. 2. Photographs of a 28-year-old female patient with cellulite from oblique and posterior views. *Blue* and *gray* lines indicate the location of the incisions for the transverse and longitudinal sections (*blue*, transverse; *gray*, longitudinal). Note how the cellulite is only present below the *red dotted line* (the level of the coccygeal-sacral fusion) (i.e., in the inferior quadrants of the gluteal region).

row located in (1) the most superficial layer of the superficial fat and (2) the most superficial layer of deep fat (Figs. 3 and 4).

3. Thickness of fatty layers (in millimeters): the total thickness of the superficial and deep fatty layers.

Fat lobule number was counted over a 3-cm length. Fat lobule height and total thickness of the respective fatty layers were measured at 0, 1.5, and 3 cm of the 5-cm full-thickness incisions, and averages were used for further statistical analyses. Fat lobule width was determined by dividing the length of the section of interest (3 cm) by the

counted fat lobule number. All measurements were conducted and verified by two independent observers (C.R. and C.H.).

Measurements of the Force to Cause Septal Breakage

To measure the minimum force required to cause septal breakage in the superficial fatty layer, the tissue at each incision was excised as a section with uniform thickness (5×1 cm). Two absorbable, undyed, braided 1-0 Vicryl sutures (Ethicon, Inc., Somerville, N.J.) were then placed 3 cm apart, looping around the dermis (superior sutures) and around the superficial fascia (inferior sutures). A

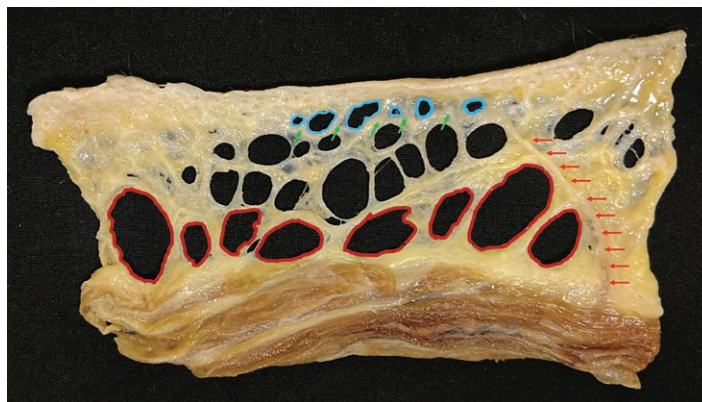


Fig. 3. Photograph of a longitudinal slice of a 72-year-old female cadaver with a body mass index greater than 30 kg/m^2 . Large fat lobules are present in the deep layer of the slice (encircled in red) below the superficial fascia. Subdermal lobules are smaller (encircled in blue) and round. Two types of septa are noted. The green arrows indicate the numerous thin, short septa separating each fat lobule and connecting the superficial fascia to the dermis. The red arrows indicate a long fibrous septal connection that extends from deep fascia to the dermis and encases an accompanying artery, vein, and nerve bundle.

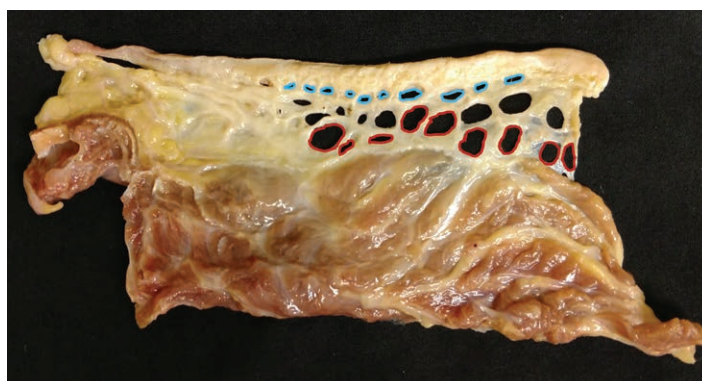


Fig. 4. Photograph of a longitudinal slice of an 80-year-old male cadaver with a body mass index less than 30 kg/m^2 . There are numerous oblique-shaped, small, subdermal fat lobules (encircled in blue) in the superficial layer and larger lobules (encircled in red) in the deep layer. Note the increased number of fat lobules and septal connections.

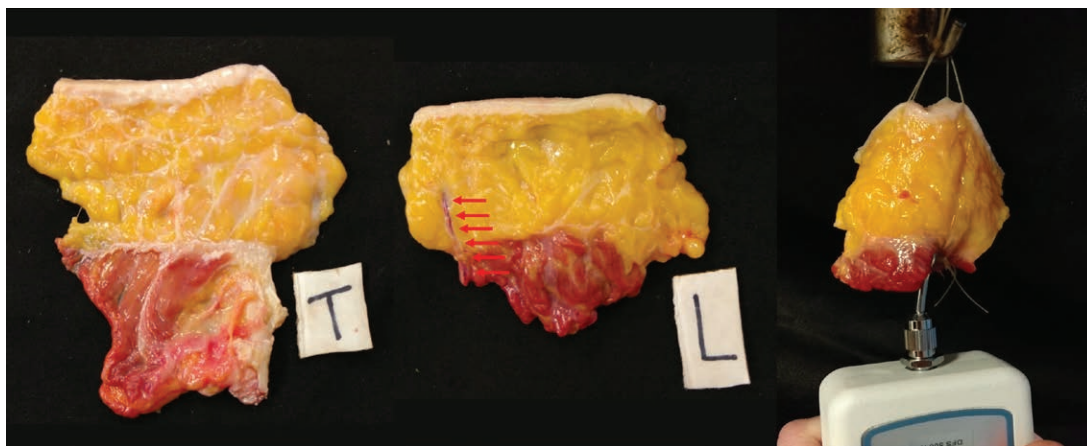


Fig. 5. (Left and center) Photograph depicting a transverse slice (T) and a longitudinal slice (L). Note the neurovascular bundle apparent in the longitudinal slice (red arrows). (Right) The DFS500 force gauge was used to measure the force required for septal breakage by attaching it to the respective slices.

steadily increasing force was applied to distend the superior from the inferior sutures and cause septal breakage in the superficial fatty layer. The minimum force was measured and documented in newtons using a Nextech DFS500 Digital Force Gauge (Nextech Systems, LLC, Tampa, Fla.) (Fig. 5). All measurements were performed by the same investigator (C.R.) and verified for consistency by a second observer (C.H.).

Statistical Analyses

Differences between values obtained in male versus female body donors were calculated using unpaired *t* tests. Paired *t* tests were used to compare values of the fatty layers. Correlations between the force needed to cause septal breakage and structural parameters (height and width) measured in the longitudinal and transverse sections were calculated by the Pearson correlation coefficient (r_p) using bivariate correlations. To identify the influence of age, sex, and body mass index, adjusted generalized linear models with robust estimators were performed reporting the odds ratio and the 95 percent confidence interval. All analyses were performed using IBM SPSS Version 23 (IBM Corp., Armonk, N.Y.), and results were considered significant for values of $p \leq 0.05$.

RESULTS

Superficial to the gluteus maximus muscle, five different layers were consistently identified in both sexes: dermis, superficial fat, superficial fascia, deep fat, and deep fascia (Fig. 1). In addition, two different types of septa were observed: numerous short, thin septa connecting the superficial

fascia to the dermis; and fewer long, thick septa spanning from the deep fascia to the dermis and carrying neurovascular bundles (Figs. 3 and 6 through 8).

The superficial fatty layer had a significantly higher number (8.78 ± 2.8 versus 4.74 ± 1.4 ; $p < 0.001$), smaller height (2.98 ± 1.3 mm versus 4.85 ± 2.7 mm; $p < 0.001$), and smaller width (3.81 ± 1.3 mm versus 7.05 ± 2.7 mm; $p < 0.001$) of honeycomb-arranged subdermal fat lobules compared with the deep fatty layer (Figs. 1, 3, and 4). This trend was consistently seen in both sexes during stratified comparisons (all $p < 0.01$). The deep layer was significantly thicker than the

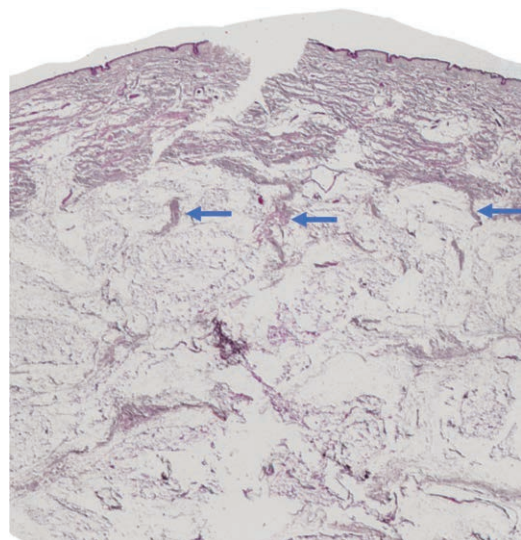


Fig. 6. Hematoxylin and eosin–stained histologic slide of the gluteal subdermal region (2-cm section) of a female cadaver. Blue arrows indicate the thin connective tissue fibers inserting into the dermis.

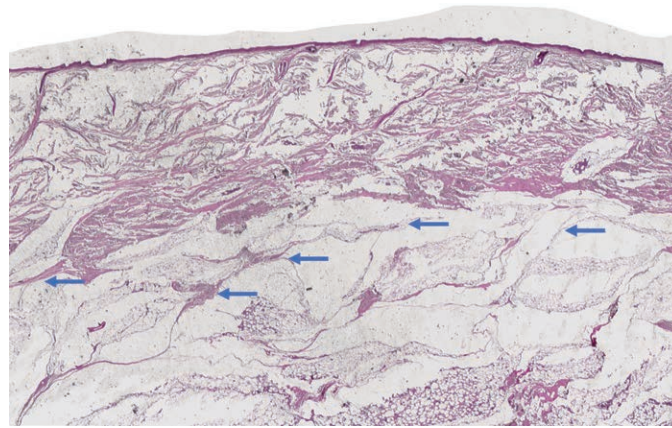


Fig. 7. Hematoxylin and eosin–stained histologic slide of the gluteal subdermal region (2-cm section) of a male cadaver. Blue arrows indicate the thin connective tissue fibers inserting into the dermis.

superficial fatty layer (12.46 ± 5.7 mm versus 7.33 ± 3.8 mm; $p < 0.001$) (Fig. 1). An increase in body mass index was significantly correlated with an increased thickness of the superficial fat ($r = 0.52$; $p = 0.001$) and the deep fat ($r_p = 0.70$; $p < 0.001$) (Figs. 9 and 10).

The mean dermal thickness was not significantly different between male cadavers versus female cadavers (1.70 ± 0.7 mm and 1.73 ± 0.8 mm; $p = 0.903$). Increased age (OR, 0.997; 95 percent CI, 0.996 to 0.998; $p < 0.000$), but not increased body mass index (OR, 1.00; 95 percent CI, 0.99 to 1.00; $p = 0.904$), was significantly related to decreased dermal thickness (OR, 0.997;

95 percent CI, 0.996 to 0.998; $p < 0.000$), indicating that increased age leads to dermal thinning by 0.3 percent per year independent of sex and body mass index.

Mean fat lobule number in the first row of the superficial fatty layer was significantly higher in male body donors (10.05 ± 2.3) compared with female body donors (7.51 ± 2.7) ($p = 0.003$) (Figs. 3, 4, 6, and 7). This number was influenced by male sex (OR, 12.70; 95 percent CI, 2.27 to 71.08; $p = 0.004$), but not by an increased body mass index (OR, 1.00; 95 percent CI, 0.87 to 1.15; $p = 0.972$) or age (OR, 0.99; 95 percent CI, 0.95 to 1.03; $p = 0.651$). This indicates that male sex is associated with a greater fat lobule number and thus a greater number of septal connections per measured area in the first row of the superficial fatty layer. In this layer, fat lobule height was significantly higher in female than in male body donors (3.64 ± 1.3 mm versus 2.32 ± 0.9 mm; $p = 0.001$). Female body donors also had a significantly greater fat lobule width in this layer than male body donors (4.44 ± 1.4 mm versus 3.17 ± 0.9 mm; $p = 0.001$). Therefore, female sex contributed significantly to increased fat lobule height (OR, 1.10; 95 percent CI, 1.02 to 1.17; $p = 0.011$) and width (OR, 1.14; 95 percent CI, 1.05 to 1.23; $p = 0.002$). Conversely, an increase in body mass index significantly influenced fat lobule height (OR, 1.01; 95 percent CI, 1.00 to 1.01; $p = 0.031$) but not width (OR, 1.00; 95 percent CI, 0.99 to 1.01; $p = 0.967$) in the superficial fatty layer. Other gender differences are listed in Table 1.

In the first row of fat lobules located immediately deep to the superficial fascia (i.e., within the deep fatty layer), the average fat lobule number

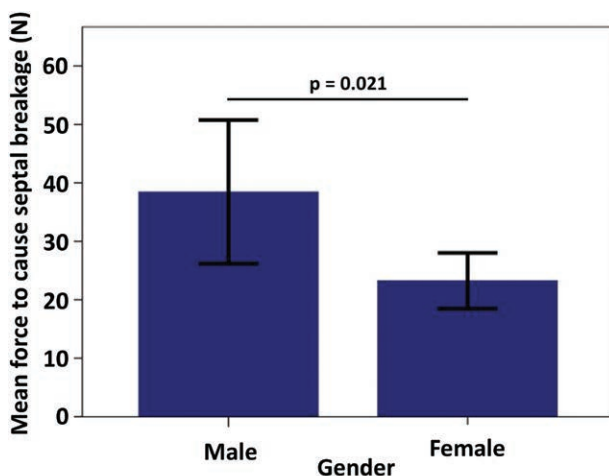


Fig. 8. Bar graph depicting the mean force required to cause septal breakage (in newtons) in male and female body donors. Septal breakage in male body donors required a statistically significant higher force on average than septal breakage in female body donors ($p = 0.021$). Error bars = 95 percent CI.

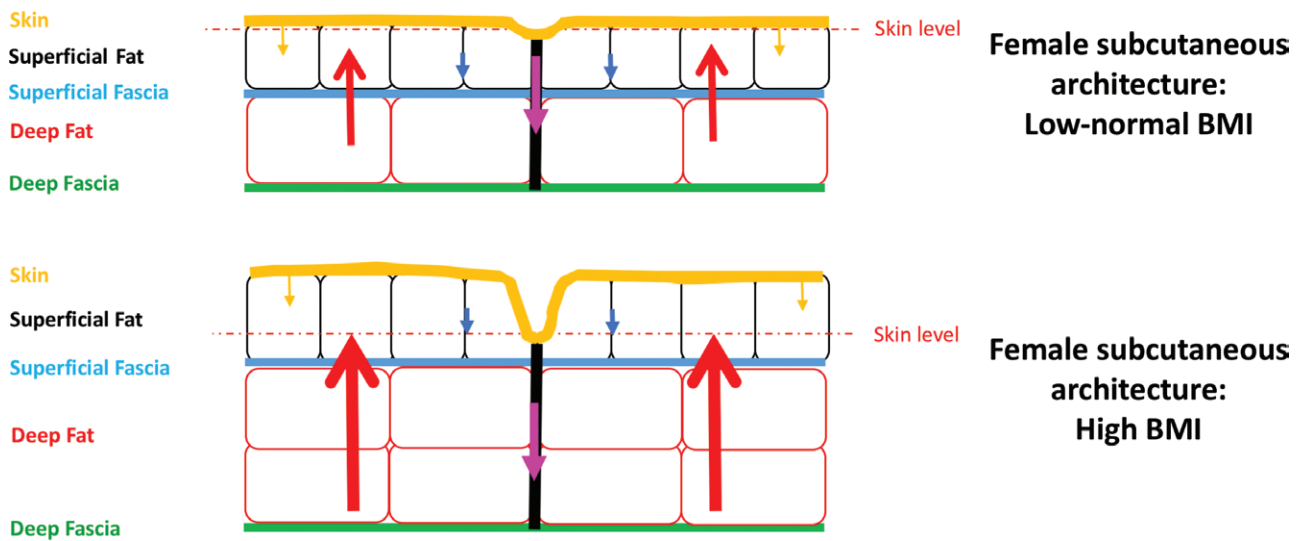


Fig. 9. Schematic illustration depicting the new postulated mechanism of action. (Above) The structure and arrangement of the skin and subcutaneous tissue of female body donors with a low-normal body mass index (*BMI*) is depicted. From superficial to deep, the dermis, superficial fat, superficial fascia, deep fat, and deep fascia are depicted. The *arrows* demonstrate the resultant interplay of biomechanical forces: the *red arrows* illustrate the outward force of the fat lobules, the *lavender arrow* and *blue arrows* illustrate the inward tethering force of the septal network [with illustrated dimorphism between the numerous, short, thin septa (*blue arrows*) versus the fewer long and thick septa, which have greater stability (*lavender arrow*)], and the *yellow arrows* depict the inward, containment force of the dermis. The low-normal body mass index woman depicted may or may not have clinical cellulite as a result of imbalance of these forces because of the fewer short septal connections being unable to contain the tall superficial fat lobules, thereby creating a dimple at the inflexible thick septal connection. (Below) The subcutaneous tissue in a female body donor with a high body mass index is shown. As body mass index increases, the height of the superficial fat lobules and the thickness of both fatty layers increases, exaggerating the imbalance of forces at the subdermal junction. This is likely to result in the clinical appearance of more severe cellulite (i.e., a mattress appearance at the skin surface).

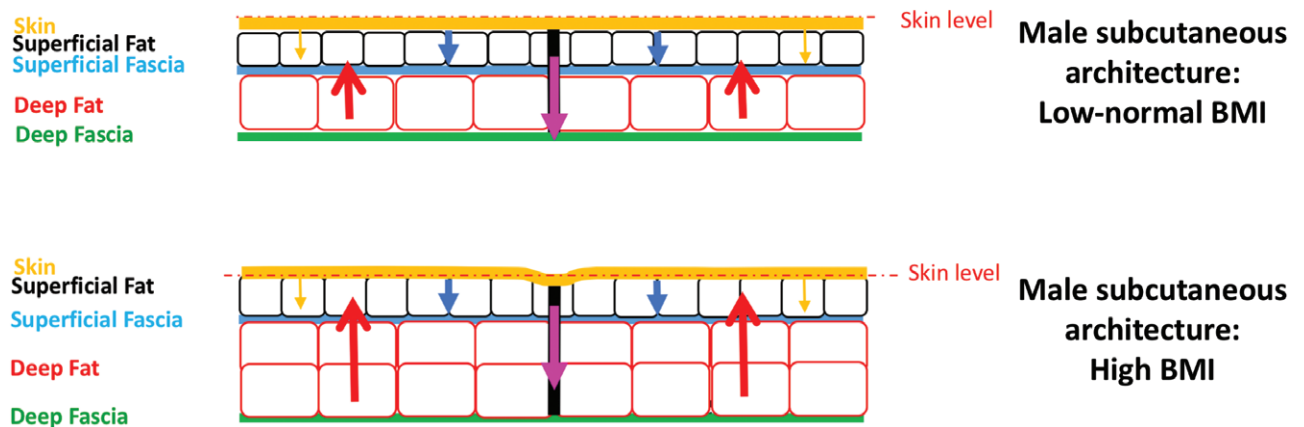


Fig. 10. Schematic illustration depicting the layered arrangement of the skin and subcutaneous tissues of male subjects with normal body mass index (*BMI*) (above) and of obese male subjects (below). The *arrows* demonstrate the resultant interplay of biomechanical forces: the *red arrows* illustrate the outward force of the fat lobules, the *lavender arrow* and *blue arrows* illustrate the inward tethering force of the septal network [with illustrated dimorphism between the numerous, short, and thin septa (*blue arrows*) versus the fewer long and thick septa, which have greater stability (*lavender arrow*)]; the *yellow arrows* depict the inward, containment force of the dermis. Because of the greater number of fibrous connections between the superficial fascia and the dermis than in female subjects, more stability is provided in male body donors, resulting in a decreased probability of a mattress-like appearance at the skin surface seen in cellulite. In the top illustration of a low-normal body mass index male subject, the clinical appearance of cellulite is unlikely. As the body mass index increases, the height of superficial fat lobules and the thickness of both fatty layers increases. The more obese male subject is less prone than an obese female subject to the appearance of cellulite because of the increased stability and inward force provided by the higher number of septal connections. An obese male subject may be less likely to demonstrate the appearance of cellulite.

was not significantly different between sexes (male body donors, 5.06 ± 1.4 ; female body donors, 4.42 ± 1.4 ; $p = 0.158$) (Figs. 3, 4, 6, and 7). Compared with male body donors, female body donors had a significantly larger fat lobule height (5.80 ± 3.0 mm versus 3.89 ± 1.9 mm; $p = 0.022$), but not width (7.60 ± 2.8 mm versus 6.52 ± 2.5 mm; $p = 0.207$). Adjusted generalized linear models revealed that neither sex nor body mass index significantly influenced the architectural arrangement, consisting of the number, height, and width of fat lobules, and in turn, septal number (all $p > 0.05$).

A significantly greater force was required to cause septal breakage within the superficial fat in male body donors compared with female body donors (38.46 ± 26.3 N versus 23.26 ± 10.2 N; $p = 0.021$) (Fig. 8). Adjusted generalized linear models revealed that body mass index did not significantly influence this relationship (OR, 0.93; 95 percent CI, 0.36 to 2.43; $p = 0.885$). Independent of sex or body mass index, longitudinal sections needed less force to cause septal breakage (26.97 ± 17.4 N) than transverse sections (34.74 ± 24.1 N) ($p = 0.250$). Fat lobule height (but not the width) in a longitudinal section was inversely correlated with the force needed to cause septal breakage ($r_p = -0.45$; $p = 0.045$). This relationship was not as prominent in transverse sections ($r_p = -0.39$; $p = 0.093$). Section orientation was not associated with any other significant differences in measured architectural parameters (data not shown).

DISCUSSION

This study investigated sex-specific differences in the architectural arrangement of the gluteal subcutaneous tissue and related biomechanical properties. Using full-thickness sections, we identified five different layers overlying the gluteus maximus muscle (dermis, superficial fat, superficial fascia, deep fat, and deep fascia) (Fig. 1) and two different types of septa (numerous short, thin septa connecting the superficial fascia to the dermis and fewer long, thick septa linking the deep fascia to the dermis and carrying neurovascular bundles) (Figs. 3, 6, and 7). Both the superficial and deep fatty layers formed a honeycomb-like structure of fat lobules enclosed by fibrous connective tissue. Independent of sex, the superficial fatty layer had a greater number and smaller (both height and width) fat lobules compared with the deep fatty layer. Sections obtained from female donors had significantly fewer fat lobules, and these fat lobules

were also greater in height and width compared with those seen in male donors; these differences were more prominent in the superficial fatty layer than in the deep fatty layer (Table 1 and Figs. 3 and 4). Increased body mass index was associated with increased fat lobule height in the superficial layer, but not fat lobule width or number, or any structural parameter measured in the deep fatty layer; however, overall thickness of both fatty layers increased significantly with higher body mass index. Dermal thickness was not significantly different between sexes but decreased with increasing age, independent of body mass index. The force necessary to cause tissue disruption between the dermis and superficial fascia was significantly higher in male body donors than in female body donors and was not influenced by body mass index (Fig. 8). Increased fat lobule height (seen in female body donors and donors with a higher body mass index) was associated with a reduced force to cause septal breakage, which was significant for the longitudinal sections but not for transverse sections.

The strength of this work is that, for the first time in cellulite research, a correlation is established between the subcutaneous tissue structural arrangement and the biomechanical properties inherent in this architecture. We identified that male body donors have a higher subcutaneous fat lobule number per given area and a greater fibrous band number in the same area. We also identified that male body donors required a significantly greater force to disrupt the fibrous connections between the dermis and the superficial fascia compared with female body donors (Fig. 8). From a biomechanical perspective, we believe that these differences in the subcutaneous fat structural arrangement are directly related to the differences in force required to rupture the fibrous bands. The greater biomechanical stability noted in male body donors, compared with female body donors, then is attributable to the architectural arrangement differences of that subcutaneous fat (Figs. 9 and 10).

Our results revealed a significant dermal thinning by 0.3 percent per year independent of sex and body mass index. A thinner dermis in aged individuals provides less support to contain the underlying soft tissues.^{14,31-33}

Our study revealed that high body mass index significantly increases the thickness of both fatty layers, and correlates to an increase in the fat lobule height in the superficial layer only. These increases could lead to an imbalance between the containing forces of the dermis and fibrous

connective tissue and the expansion of both fatty layers (Figs. 9 and 10).

Our observations also revealed two distinct fibrous septal types: short and thin septa, which are numerous; and long and thick septa, which were fewer. The short, thin septa connected the dermis to the superficial fascia; this plane was the consistent point of rupture during biomechanical testing and therefore the area most responsible for biomechanical stability. The long, thick septa also spanned this plane but originated from the deep fascia and were accompanied by neurovascular bundles. Because of the cadaveric nature of this investigation, the study sample consisted of aged male and female body donors with a mean age of 76 ± 16.47 years (range, 36 to 92 years); this can be considered as a limitation of this study. Independent of sex and age, however, we observed a patent vasculature; this may explain the high rate of bruising seen after subcision procedures (i.e., the transection of subdermally located fibrous septa) for cellulite treatment.^{9,34} Contrary to previous studies, this patent vasculature also supports the concept that these long septa are not sclerosed.^{10,18,25,35}

One limitation of this study was sample size: only 10 male and 10 female body donors were studied. Furthermore, the female donors had a significantly higher body mass index (Table 1) compared with the male body donors. We generated 40 observations, however, by collecting data from both longitudinal and transverse sections. To avoid interpretational bias, for all statistical analyses, we performed adjusted multifactorial testing to account for body mass index–related differences.

In summary, our observations reveal an interplay of the structural characteristics and the biomechanical properties at the subdermal junction (i.e., between the dermis and the subcutaneous fat). This interactive relationship between the support offered by the dermis, the type and number of septal connections, and the architecture of the superficial and the deep fatty layers determines the presence or absence of cellulite (Figs. 9 and 10). This delicate balance is further influenced by sex, increasing age, and high body mass index—which are all recognized cellulite risk factors.^{5,25,27,33,36,37} Women at any age and with any body mass index are inherently at greater risk for developing cellulite than men because of their reduced septal number and increased superficial fat lobule height. Our results demonstrated that these structural factors lead to a significantly reduced biomechanical stability in women compared with men.

Increased age resulted in a significant thinning of the dermis independent of sex, providing less support to contain the underlying fatty layers. These findings are in line with clinical observations in which increased age and skin laxity are related to an increased prevalence and/or worsening of cellulite.^{14,31–33,38} High body mass index resulted in an increase in the thickness of both the superficial and the deep fatty layers and also an increase in fat lobule height in the superficial fatty layer. These increases could upset the delicate balance between containment and extrusion forces at the subdermal junction that favor extrusion. Together with an increase in biomechanical instability attributable to fewer septal connections, increased fat lobule height, and thinner skin, obese, aged women are highly predisposed to the presence and worsening of cellulite. The dimorphism observed in septal morphology may contribute to the mattress-like appearance in cellulite.

CONCLUSIONS

Cellulite can be understood as an imbalance between the delicate containment and extrusion forces at the subdermal junction. Because of the interaction of the architectural arrangement of the superficial and deep fatty layers with the biomechanical properties and dimorphism of the fibrous septa, aged women, with higher body mass indexes, have the greatest risk of developing cellulite or having cellulite of higher grade. Therapeutic options targeting cellulite should aim to strengthen the subdermal interface and/or to release the fibrous septa by means of various types of subcision.

Sebastian Cotofana M.D., Ph.D.

Albany Medical College

47 New Scotland Avenue, MC-135

Albany, N.Y. 12208

cotofas@mail.amc.edu

Instagram: @professorsebastiancotofana

Facebook: professorsebastiancotofana

ACKNOWLEDGMENTS

The authors would like to thank Lisa D. Parr for continuous support of their theory, Gerardo Escobar and Simone Arnold for statistical expertise during the authors' analyses, and Prof. Alfredo Jacomo and Dr. Flavio Hojaij from the University of Sao Paulo for the histologic samples.

REFERENCES

1. Hexsel D, Camozzato FO, Silva AF, Siega C. Acoustic wave therapy for cellulite, body shaping and fat reduction. *J Cosmet Laser Ther.* 2017;19:165–173.

2. Soares JL, Miot HA, Sanudo A, Bagatin E. Cellulite: Poor correlation between instrumental methods and photograph evaluation for severity classification. *Int J Cosmet Sci*. 2015;37:134–140.
3. Hexsel D, Hexsel C, Weber M. Social impact of cellulite and its impact on quality of life. In: Goldman M, Hexsel D, eds. *Pathophysiology and Treatment (Basic Clinical Dermatology)*. 2nd ed. Boca Raton, Fla: CRC Press; 2010:1–5.
4. Rawlings AV. Cellulite and its treatment. *Int J Cosmet Sci*. 2006;28:175–190.
5. Nürnberger F, Müller G. So-called cellulite: An invented disease. *J Dermatol Surg Oncol*. 1978;4:221–229.
6. Emanuele E. Cellulite: Advances in treatment. Facts and controversies. *Clin Dermatol*. 2013;31:725–730.
7. Avram MM. Cellulite: A review of its physiology and treatment. *J Cosmet Laser Ther*. 2004;6:181–185.
8. Luebberding S, Krueger N, Sadick NS. Cellulite: An evidence-based review. *Am J Clin Dermatol*. 2015;16:243–256.
9. Friedmann DP, Vick GL, Mishra V. Cellulite: A review with a focus on subcision. *Clin Cosmet Investig Dermatol*. 2017;10:17–23.
10. Rossi AB, Vergnanini AL. Cellulite: A review. *J Eur Acad Dermatol Venereol*. 2000;14:251–262.
11. Rao J, Gold MH, Goldman MP. A two-center, double-blinded, randomized trial testing the tolerability and efficacy of a novel therapeutic agent for cellulite reduction. *J Cosmet Dermatol*. 2005;4:93–102.
12. Draeos ZD, Marenus KD. Cellulite: Etiology and purported treatment. *Dermatol Surg*. 1997;23:1177–1181.
13. Callaghan DJ III, Robinson DM, Kaminer MS. Cellulite: A review of pathogenesis-directed therapy. *Semin Cutan Med Surg*. 2017;36:179–184.
14. Hexsel D, Siega C, Schilling-Souza J, Porto MD, Rodrigues TC. A comparative study of the anatomy of adipose tissue in areas with and without raised lesions of cellulite using magnetic resonance imaging. *Dermatol Surg*. 2013;39:1877–1886.
15. Manuskiatti W, Wachirakaphan C, Lektrakul N, Varothai S. Circumference reduction and cellulite treatment with a TriPollar radiofrequency device: A pilot study. *J Eur Acad Dermatol Venereol*. 2009;23:820–827.
16. Kruglikov I. The pathophysiology of cellulite: Can the puzzle eventually be solved? *J Cosmet Dermatol Sci Appl*. 2012;2:1–7.
17. Emanuele E, Minoretta P, Altabas K, Gaeta E, Altabas V. Adiponectin expression in subcutaneous adipose tissue is reduced in women with cellulite. *Int J Dermatol*. 2011;50:412–416.
18. Curri S. Cellulite and fatty tissue microcirculation. *Cosmet Toilet*. 1993;108:51–58.
19. Terranova F, Berardesca E, Maibach H. Cellulite: Nature and aetiopathogenesis. *Int J Cosmet Sci*. 2006;28:157–167.
20. Piérard GE. Commentary on cellulite: Skin mechanobiology and the waist-to-hip ratio. *J Cosmet Dermatol*. 2005;4:151–152.
21. de Godoy JM, de Godoy Mde F. Physiopathological hypothesis of cellulite. *Open Cardiovasc Med J*. 2009;3:96–97.
22. Rosenbaum M, Prieto V, Hellmer J, et al. An exploratory investigation of the morphology and biochemistry of cellulite. *Plast Reconstr Surg*. 1998;101:1934–1939.
23. Querleux B, Cornillon C, Jolivet O, Bittoun J. Anatomy and physiology of subcutaneous adipose tissue by in vivo magnetic resonance imaging and spectroscopy: Relationships with sex and presence of cellulite. *Skin Res Technol*. 2002;8:118–124.
24. Hexsel DM, Abreu M, Rodrigues TC, Soirefmann M, do Prado DZ, Gamboa MM. Side-by-side comparison of areas with and without cellulite depressions using magnetic resonance imaging. *Dermatol Surg*. 2009;35:1471–1477.
25. Piérard GE, Nizet JL, Piérard-Franchimont C. Cellulite: From standing fat herniation to hypodermal stretch marks. *Am J Dermatopathol*. 2000;22:34–37.
26. Quatresooz P, Xhaufaire-Uhoda E, Piérard-Franchimont C, Piérard GE. Cellulite histopathology and related mechanobiology. *Int J Cosmet Sci*. 2006;28:207–210.
27. Mirrashed F, Sharp JC, Krause V, Morgan J, Tomanek B. Pilot study of dermal and subcutaneous fat structures by MRI in individuals who differ in gender, BMI, and cellulite grading. *Skin Res Technol*. 2004;10:161–168.
28. Omi T, Sato S, Kawana S. Ultrastructural assessment of cellulite morphology: Clues to a therapeutic strategy? *Laser Ther*. 2013;22:131–136.
29. Emanuele E, Bertona M, Geroldi D. A multilocus candidate approach identifies ACE and HIF1A as susceptibility genes for cellulite. *J Eur Acad Dermatol Venereol*. 2010;24:930–935.
30. Hexsel DM, Dal'forno T, Hexsel CL. A validated photonumeric cellulite severity scale. *J Eur Acad Dermatol Venereol*. 2009;23:523–528.
31. Christ C, Brenke R, Sattler G, Siems W, Novak P, Daser A. Improvement in skin elasticity in the treatment of cellulite and connective tissue weakness by means of extracorporeal pulse activation therapy. *Aesthet Surg J*. 2008;28:538–544.
32. Ortonne JP, Zartarian M, Verschoore M, Queille-Roussel C, Duteil L. Cellulite and skin ageing: Is there any interaction? *J Eur Acad Dermatol Venereol*. 2008;22:827–834.
33. Leszko M. Cellulite in menopause. *Prz Menopauzalny*. 2014;13:298–304.
34. Hexsel DM, Mazzuco R. Subcision: A treatment for cellulite. *Int J Dermatol*. 2000;39:539–544.
35. Alster TS, Tehrani M. Treatment of cellulite with optical devices: An overview with practical considerations. *Lasers Surg Med*. 2006;38:727–730.
36. Smalls LK, Lee CY, Whitestone J, Kitzmiller WJ, Wickert RR, Visscher MO. Quantitative model of cellulite: Three-dimensional skin surface topography, biophysical characterization, and relationship to human perception. *J Cosmet Sci*. 2005;56:105–120.
37. De La Casa Almeida M, Suarez Serrano C, Rebollo Roldán J, Jiménez Rejano JJ. Cellulite's aetiology: A review. *J Eur Acad Dermatology Venereol*. 2013;27:273–278.
38. Dobke MK, Dibernardo B, Thompson RC, Usal H. Assessment of biomechanical skin properties: Is cellulitic skin different? *Aesthet Surg J*. 2002;22:260–266.